RESEARCH ARTICLE

Sampling Procedure, Characterization, and Quantitative Analyses of Industrial Aluminum White Dross

Cathrine Kyung Won Solem[1] · Stefano Deledda[2] · Gabriella Tranell[1] · Ragnhild E. Aune[1]

Abstract
Up to 10% of all metallic aluminum (Al) produced is lost due to dross generation during production. It also causes an environmental problem due to hazardous waste generation following treatment, as well as toxic gas generation when in contact with water/humidity. As a result, it is desirable to identify the parameters contributing to the generation of the Al white dross mixture. In view of this, a sampling procedure for collecting representative dross samples directly from the casthouse holding furnace has been developed together with a methodology for analyzing and evaluating the results. XRD was used for phase/chemical composition analyses of sieved dross samples, and both ring milling and cryomilling were used during sample preparation. Cryomilling proved to be the superior method allowing dross fractions < 1.25 and 1.25–4.5 mm to be pulverized. The fractions were analyzed and revealed that the sampling location inside the furnace plays a vital role as the injection of primary-produced Al into the furnace influences the dross characteristics. From Location 1 (closest to the injection point) to Location 4 (furthest away from the injection point), the metallic Al content in the dross decreased simultaneously as the oxide content increased. The results also confirmed that the larger size fraction had a higher metallic Al concentration, which correlates well with literature findings. By adopting a methodical sampling procedure followed by consistent routines for sample preparation, characterization, and analyses, process operations can be studied and thereby potentially used to minimize the loss of Al due to dross formation.

Graphical Abstract
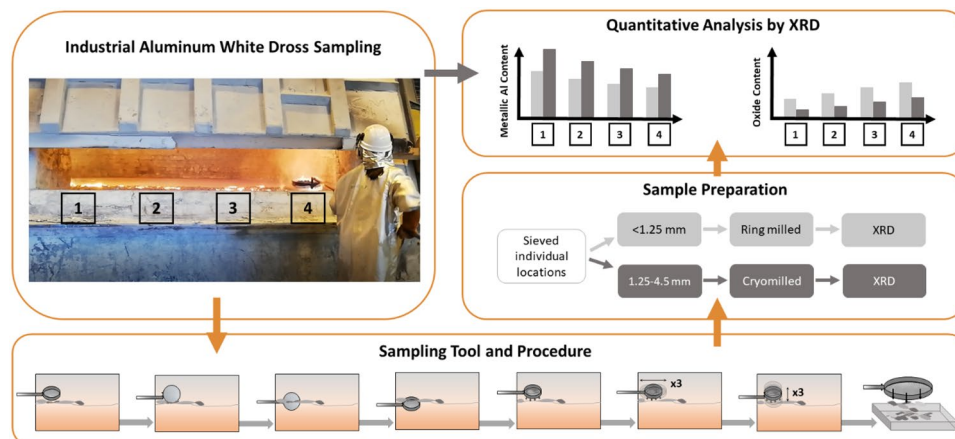
Keywords Aluminum dross · Sampling · Cryomilling · XRD · Rietveld method

Introduction

Aluminum (Al) is the second most important metal in modern society [1, 2], and the metal is carefully treated during production to obtain the desired characteristics of the product, e.g., the required cleanliness, to tailor properties such as weldability, strength, and formability [3, 4]. Al is produced via both primary and secondary routes, and both routes generate side streams such as Al dross, which is a mixture of metallic Al, Al oxides, and oxides of alloying elements in addition to carbide and/or nitride compounds of these metals [5].

It is a well-known fact that Al has a high oxygen affinity and that the oxidation of Al is an exothermic reaction forming Al oxide (Al_2O_3) [6]. This means that during processing in the casthouse, there will always be a loss of Al when the Al oxide film formed on the surface of the molten metal is disturbed and broken up due to furnace operations such as during stirring and melt transfer operations [7].

During one-furnace practice (where melting of scrap, injection of primary-produced Al, stirring and skimming is performed in the same furnace), the injection of primary-produced Al is a critical process step as the injection influences the turbulence of the melt from one specific side of the furnace [8]. The same flow is, however, not seen during the two-furnace practice, as the melt is transferred from one furnace to another from the center-back of the furnace, causing a more symmetric melt distribution. Typical for both operations is that the melt must be stirred and skimmed before casting, which generates dross consisting of accumulated oxides together with metallic Al entrained within the oxide films and Non-Metallic Compounds (NMC) [8, 9]. Due to dross generation, as much as 10% of the annual primary production of metallic Al has been reported to be lost [10, 11]. The dross generated during primary production of Al is defined as white dross and can potentially contain up to 70–75% metallic Al in addition to the Al lost due to oxidation [2, 10].

Aluminum dross is a hazardous waste due to its reactivity when in contact with humidity or water [2, 12]. Toxic gases such as phosphine (PH_3), ammonia (NH_3), methane (CH_4), and hydrogen sulfide (H_2S) may be generated, which can cause both human and environmental harm during unit operations such as dross storage, transport, and in some countries when landfilled [12, 13]. It is, therefore, desirable to reduce the dross generation during Al production to improve the metallic yield, as well as to lower the negative environmental load.

The heterogeneity of Al white dross makes it challenging to determine how different parameters, such as temperature, atmosphere, furnace operations, and chemical composition, influence the amount of dross generated and

its characteristics. The present work has therefore sought to establish a methodology where Al white dross can be systematically collected directly from the holding furnaces in the casthouse and further analyzed. By adopting the method, the work also aims to determine the influence of standard furnace operations on dross generation, as well as how the sampling location inside the furnace influences the properties of the dross and the amount of entrained metallic Al.

Industrial Sampling Technique

Several studies dealing with the challenges of Al white dross collection and analyses can be found in the literature [14, 15]. However, as many of these studies characterize the dross, and report on their metallic Al concentration, see Table 1, the outcome of these studies varies. It has therefore been challenging to extract how the samples have been collected, analyzed, and further used to improve process operations [16–20].

Sampling Equipment and Procedure

The state-of-the-art for removing floating oxides and other NMC from the surface of molten Al is to manually use a metal rake (generally referred to as skimming, see Fig. 1a). The removed dross is, in this case, collected directly into an open bin in front of the furnace, see Fig. 1b. However, the collection of dross samples is not part of the routine of furnace operation and is only sampled sporadically whenever needed. This could be when unusual behavior is seen, e.g., when the gases generated while stirring the melt self-ignite [19].

From observations made during industrial campaigns by the corresponding authors and conversations with the operators from different Al producers, it has been established that the total amount of dross generated during production is weighted after each skimming. The amount of dross generated is used to evaluate if the operational conditions set for that specific melt are optimal, i.e., the loss of metallic

Table 1 Examples of studies and the metallic Al content in the white dross

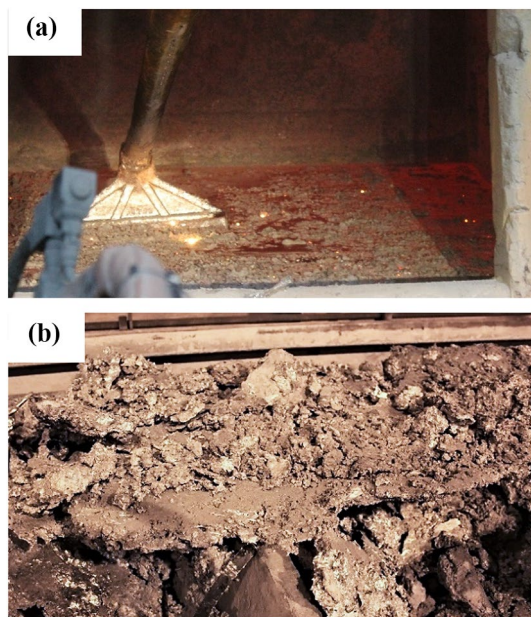| Metallic Al content in the dross, /wt.%	Reference
42.52	Abdulkadir et al. [16]
43.30	David and Kopac [17]
43.40	Hwang et al. [18]
55.70	Capuzzi and Timelli [19]
74.08	Meshram et al. [20]

Fig. 1 a Non-Metallic Compounds (NMC) being removed (skimmed off) from a molten aluminum (Al) melt. **b** Skimmed-off white Al dross consisting of large flakes, lumps, particles, and dust left for cooling

Fig. 2 a Image of the sieve and disassembled handle used as the sampling tool to collect industrial Al white dross samples. **b** The perforated steel plate of the sieve

Al is at the lowest level possible in view of the operating conditions.

Molten Al samples are also collected to control the chemical composition of the metal. These samples are collected in a small cup submerged into the melt and then transferred to a mold shaped like a disc of 5 cm in diameter and 1 cm in height. The first sample is, by default, discarded due to the oxide skin the sampling equipment has to penetrate through during sampling, followed by two additional samples sent directly for analyses.

Quantitative Analyses

The procedure for analysis of dross samples does, however, vary. Currently, the dross treatment plant analyzes the metallic Al dross content by remelting the dross to extract the Al metal. Samples collected from dross bins have also been analyzed at external characterization sites. The dross is therefore not currently analyzed and characterized during normal production. It is, however, protocol to scale the dross bin with skimmed-off dross to control the amount of dross generated for each melt.

The molten Al samples collected are first gently sanded on both sides before being analyzed by Optical Emission Spectroscopy (OES). The obtained result is then sent to the operator in the control room station within 5–10 min from the time of co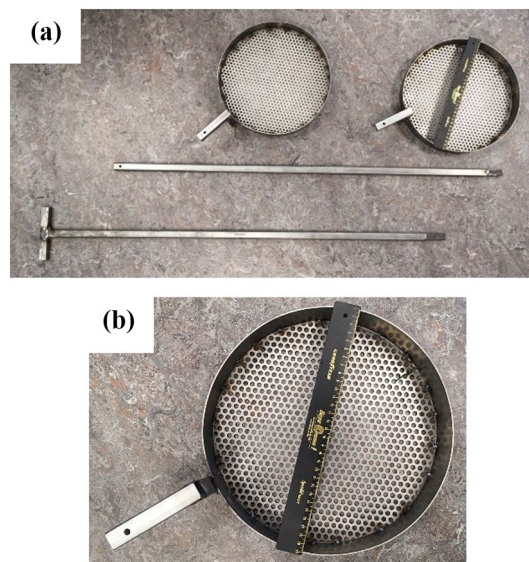llection. OES is a convenient and quick technique allowing the chemical composition of the melt to be adjusted before casting if needed.

Present Sampling Technique

Sampling Equipment and Procedure

For collecting representative dross samples from inside the holding furnace, a tool (sieve) allowing the metal to drain off as the sample was collected was designed. The diameter and height of the sieve were set to 30 and 5 cm, respectively, and a 2-m-long handle was added to allow samples to be collected from different locations in the furnace. A ¼-inch sized and 33% perforated stainless-steel plate was selected as the sieve surface, see Fig. 2a and b. The present design was inspired by a sampling device for dross used in a study reported in the literature [21], where different combinations of hole sizes and perforations of the sieve were tested.

To avoid metallic Al from sticking to the surface of the sieve during sample collection, and potentially clogging the perforated surface of the sieve, Boron Nitride (BN) spray (COBN-3, NOR) was used for coating the sieve before each sampling.

Preparation of the Furnace Melt Before Sampling

The furnace operator mixed and prepared the molten Al melt according to the following standard procedures: (i) remelting of in-house scrap, (ii) addition of primary-produced Al from the electrolysis process, and (iii) addition of alloying

elements required for the chemical composition of the alloy in question to be met. In the skimming stage, the operators paused and allowed the collection of dross (gray particles in Fig. 3a–c) that was floating on top of the hot pool of molten metal (orange areas in Fig. 3a–c).

It was, however, realized that even with a 2-m-long handle on the sieve, reaching the oxides and NMCs floating on top of the melt inside the holding furnace was challenging. Hence, the operator carefully collected the floating layer without stirring it within reach of the furnace gate, as illustrated in Fig. 3d–f. The furnace door was also lowered, leaving a gap of ~ 1 m, to minimize the heat radiation from the melt.

Collection of Dross Samples

The dross samples were collected manually using the sieve, standing in front of the molten metal bath. The sieve was gently introduced over the liquid bath, flipped 90°, and submerged directly into the hot pool of molten metal partly through the oxide/NMC (dross) layer, as illustrated in Fig. 4a–c. The sieve was flipped back 90° when submerged in the melt, see Fig. 4d, before the sieve was lifted over the dross layer. The dross/molten metal floating just above
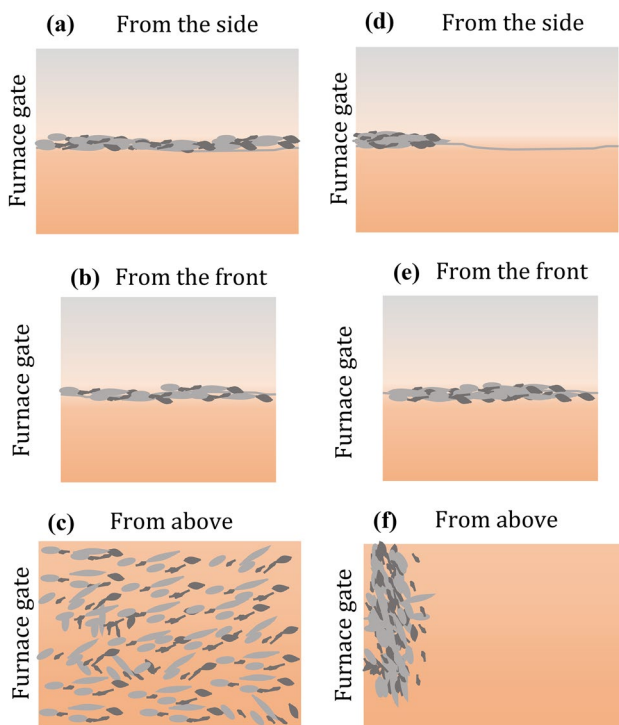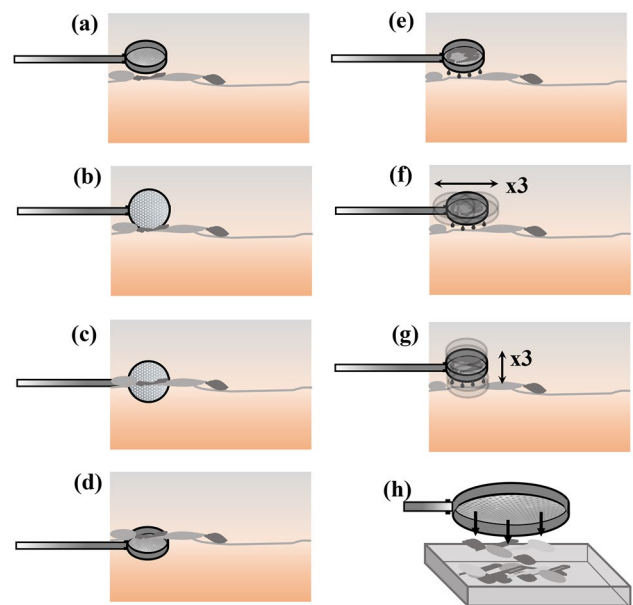

Fig. 4 Illustration of the sampling procedure of industrial Al white dross collected directly from the molten melt. The sieve is **a** introduced, **b** flipped 90°, **c** submerged into the melt, **d** flipped 90° back to a horizontal position, and **e** removed from the melt with the dross sample allowing the dross/molten metal floating just above the sieve to naturally drain off. The sieve was then shaken **f** horizontally and **g** vertically, draining off as much molten Al as possible, before being **h** transferred into a stainless-steel tray for cooling in air

the sieve was allowed to naturally drain off from the collected sample for 3 s before the sieve was shaken with a gentle force both horizontally and vertically to drain off as much molten Al as possible, i.e., the first three times horizontally and then three times vertically, see Fig. 4f–g. The collected dross sample was then transferred from the sieve into a stainless-steel tray next to the furnace, see Fig. 4h. The dross sample was then allowed to cool naturally in air to ambient temperature. Finally, after an hour, the dross sample was collected from the tray and transferred into an air-sealed container awaiting further treatment.

The same collection procedure was repeated for four different locations in the holding furnace in order to evaluate if the dross characteristics varied for different locations in the furnace. The locations were a function of distance from the primary-produced Al injection hole, see Fig. 5. As seen from the figure, Location 1 was the sampling location closest to the injection hole and Location 4 furthest away. Location 2 and Location 3 were left and right of the center, respectively.

To minimize human errors with respect to the proposed sampling technique, the same person was responsible for carrying out the dross collection for all experiments evaluated in the present work.

Fig. 3 Illustration of the hot pool of molten metal, where **a–c** shows the oxides and NMCs (gray particles) naturally distributed while floating on top of the melt (orange areas), seen from the side, the front, and above, respectively, and **d–f** when carefully collected by the furnace gate, seen from the side, the front, and above, respectively
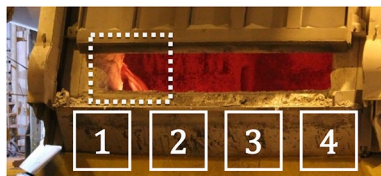
Fig. 5 Image of the front of a holding furnace in the casthouse showing the injection hole of the primary-produced Al (dashed square), as well as the four different locations from which dross samples were collected

Sample Preparation

Each collected dross sample was sieved, and the fractions < 1.25 mm and 1.25–4.5 mm were further studied. The fraction > 4.5 mm was stored for future studies. Pulverization of the collected dross samples, as well as thorough mixing of the individually obtained powders, was necessary to secure a homogeneous sample that would allow for reproducible quantitative analyses (Fig. 6).

Case Study A—Ring Milling

The dross samples were individually milled using a ring milling unit from HERZOG (HSM 100 H, Germany). The unit was equipped with Tungsten Carbide (WC) rings with an inner diameter of 60 mm and a center bolt of 38 mm.

The ring mill was cleaned by milling two rounds of 20 s with silicon oxide (SiO_2) powder and thereafter cleaned with ethanol before use. One milling cycle consisted of three sequences, each with a milling time of 20 s. The powder was sieved between each sequence, and the powder fraction with a particle size of < 100 μm was put aside. The rest of the powder was ring milled again using the same approach until reaching three sequences. Each sample had thereby a maximum milling time of 60 s.

For the smallest fraction of each dross sample, i.e., the fraction < 1.25 mm in size, the obtained powder was sieved into a sample with a particle size of < 100 μm. After sieving, each sample was stored in a glass container awaiting analysis.
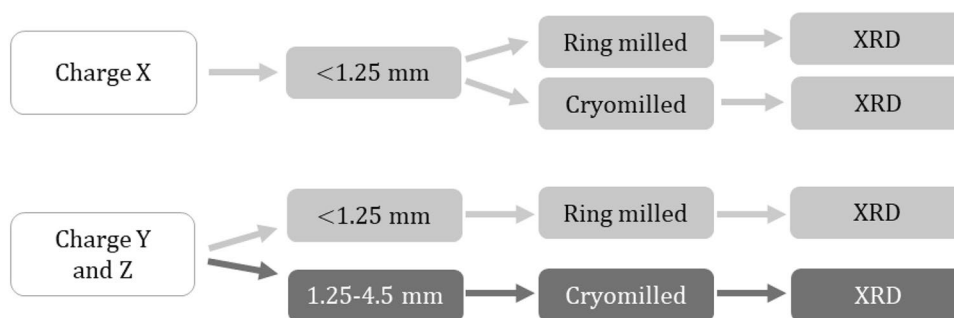
The mid-fraction of one dross sample, i.e., the fraction 1.25–4.5 mm in size, was also ring milled. However, due to its ductile properties, the metallic Al present in the samples proved to be a problem as it became deformed and stuck to the sidewalls of the ring mill. As a result, the obtained powder was partly inhomogeneous.

Case Study B—Cryomilling

The dross samples were individually crushed at Institute for Energy Technology (IFE) in Norway using a cryomilling unit from SPEX (6770 Freezer/Mill, USA). Cryomilling was performed in the vial (with a volume of 16 cm³) consisting of a central polycarbonate center cylinder and 440C steel end pieces. The cylindrical impactor was also made of 440C steel. Liquid nitrogen (N_2) was used to cool the sample down to -196 °C before and during milling. During milling, the cryomilling vial was completely submerged in a liquid N_2 bath.

The components of the cryomill vial were cleaned by sanding the impactor with sandpaper, brushed and cleaned with an abrasive detergent, and rinsed with ethanol between each milling cycle. One milling cycle consisted of a pre-cooling step of 60 min, followed by 6 min of effective cryomilling (with an impact frequency of 24 Hz) and 3 min of cooling by liquid N_2. The cryomilling was then paused to refill the liquid N_2 bath. An additional precooling step of 10 min was applied before the cryomilling was resumed to ensure reaching the target temperature (-196 °C). The procedure was repeated until a total milling time of 60 min was reached.

The mid-fractions of each dross sample (1.25–4.5 mm in size) were cryomilled, and the obtained powder was sieved into two different samples with a particle size of (i) > 100 μm and (ii) < 100 μm. In contrast to ring milling, cooling the dross with the liquid N_2 allowed the metallic Al present in the sample to embrittle and hence be crushed rather than deformed. After sieving, each sample was stored in a glass container awaiting further analyses.

Fig. 6 Flow sheet showing the different charges, fractions, and milling techniques, followed by X-Ray Diffraction (XRD) analysis

Table 2 Crystallographic information for the phases in the Al white dross, i.e., the Crystallographic Information File (CIF)

Crystalline phase		Space group	Unit cell parameters	
			a, b, c	α, β, γ
Aluminum	α-Al	F m −3 m	4.0509, 4.0509, 4.0509	90, 90, 90
Magnesium oxide	MgO	F m −3 m	4.2140, 4.2140, 4.2140	90, 90, 90
Spinel	$MgAl_2O_4$	F d −3 m	8.0830, 8.0830, 8.0830	90, 90, 90
Defect spinel [22]	$Mg_{0.388}Al_{2.408}O_4$	F d −3 m:2	7.9783, 7.9783, 7.9783	90, 90, 90
Aluminum oxide	$α-Al_2O_3$	R -3 c	4.7602, 4.7602, 12.9933	90, 90, 120
Aluminum nitride	AlN	P 63 m c	3.1114, 3.1114, 4.9784	90, 90, 120
Silicon [23]	Si	F d −3 m	5.4304, 5.4304, 5.4304	90, 90, 90
Sodium aluminum oxide	$NaAl_{11}O_{17}$	P 63 / m m c	5.5930, 5.5930, 22.6100	90, 90, 120

Quantitative Analyses

The milled and sieved samples were analyzed using an X-Ray Diffraction (XRD) unit from Bruker (D8 A25 DaVinci X-Ray Diffractometer, Billerica, USA). The unit was equipped with monochromatic CuKα radiation with a wavelength of λ = 1.5406 Å. The XRD scans were carried out with a step size of 0.020° and a step duration of 8 s/step with a fixed divergence slit of 0.100°. A scattering angle of 2θ covering a range of 6–110° was set, and an X-Ray generator of 40.0 kV was applied for all measurements.

To evaluate the results and refine the data, the TOPAS software from Bruker (version 5, Billerica, USA) was applied to refine the data. The Powder Diffraction Files (PDFs) were extracted from the ICDD-4 + PDF database. In addition, the crystallographic information for silicon (Si) and $Mg_{0.388}Al_{2.408}O_4$ (defect spinel) were obtained from literature [22, 23], see Table 2.

The TOPAS software and the ICDD-4 + PDF database were chosen for quantifying the phases, as they proved to be a suitable technique for analyzing metallic Al and the relevant oxides, e.g., MgO. A reference sample containing 50 wt.% Al and 50 wt.% MgO was prepared and analyzed using the same instrument settings as for the collected dross samples, i.e., the same step size, step duration, divergence slit, scattering angle, and voltage. The diffractogram, the fitted profile, and the difference between them are seen in Fig. 7, revealing a phase distribution of 49.9 wt.% Al and 50.1 wt.% MgO, see Table 3.

Fig. 7 XRD diffractogram of the pre-mixed reference sample containing 50 wt.% Al and 50 wt.% MgO, where the measured profile (black curve with diamonds), fitted profile by using the Rietveld Method (light gray curve), and the difference between the measured and fitted profile (dark gray curve) are plotted

Table 3 Phase distribution for the reference sample containing 50 wt.% Al and 50 wt.% MgO calculated by the Rietveld Method

Phase	Phase distribution, /wt.%
α-Al	49.9
MgO	50.1

molten metal through the holes. Based on initial observations and experiences using the sieve, it was slightly modified to meet these requirements, resulting in a perforation of 33% and both vertical and horizontal movements of the sieve before transferring the collected dross to the tray for cooling.

The sieve design and the 2-m-long handle also ensured that the metallic Al quickly drained off, avoiding clogging of the sieve. At the same time, the oxide particles entrained in the metallic Al remained in the sieve.

Sample Preparation and Analyses

Both milling techniques chosen for sample preparation for pulverization and mixing proved to work well for the smaller

Results

Sampling Equipment and Procedure

When using the sieve, it was noted that a perforation high enough to allow the metallic Al to drain both naturally and when shaken to force excess metallic Al through the holes was required. It was also noted that the holes could not be too large, allowing the smaller oxide particles to follow the
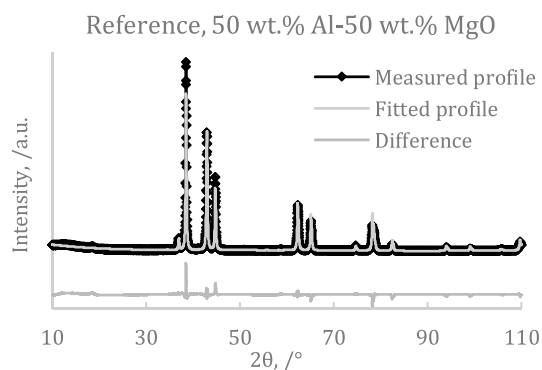
fraction of the dross (< 1.25 mm). However, cryomilling proved to be the superior method, allowing the dross to be pulverized for the smallest and mid-fractions, i.e., < 1.25 mm and 1.25–4.5 mm in size.

From the results, it was clear that by using XRD, the heterogeneous Al dross samples were allowed to be analyzed after being pulverized to a homogeneous powder. The Rietveld Method was used, as the method is well suited having a mathematical approach for fitting structural data and deconvoluting overlapping peaks, and thereby, also allowed quantification of the phase distribution by revealing the non-metallic phases.

Case Study A—Ring Milling

One ring milled < 1.25 mm pulverized dross sample (the smallest fraction) from each charge and location in the holding furnace was analyzed by XRD and quantified by the Rietveld Method. In some cases, two samples were analyzed to ensure reproducibility. Figure 8a–d presents the diffractograms and the fitted profiles from the Rietveld refinement for Locations 1 to Location 4 of Charge Y. The differences between the measured diffractograms and the calculated fitted profiles are also presented in the same figure. In Table 4, the phase distribution obtained from the refinement of the XRD patterns shown in Fig. 8 is summarized. It can be seen from the table that as the metallic Al content decreases from Location 1 to Location 4, the total oxide content increases.

Similar behavior was established for Charge Z, as seen in Table 5.

Case Study B—Cryomilling

One cryomilled 1.25–4.5 mm pulverized dross sample (mid-fraction) from each charge and location in the holding furnace was also analyzed by XRD, using the same program as for the smallest ring milled fraction. Figure 9a–d presents the diffractograms and the fitted profiles from the Rietveld refinement for Location 1 to Location 4 of Charge Y, together with the differences between the measured diffractograms and the calculated fitted profiles. In Table 6, the phase distribution obtained from the refinement of the XRD patterns presented in Fig. 9 is summarized. It can be seen from the table that as the metallic Al content decreases from Location 1 to Location 4, the total oxide content increases, which confirms the results from the ring milled samples. When comparing the metallic Al content in the mid-fraction at all four locations with the smaller fraction at the same locations, an overall higher Al concentration was obtained.

Similar behavior was also established for Charge Z, see Table 7; however, the differences between locations were clearly more noteworthy than for Charge Y.
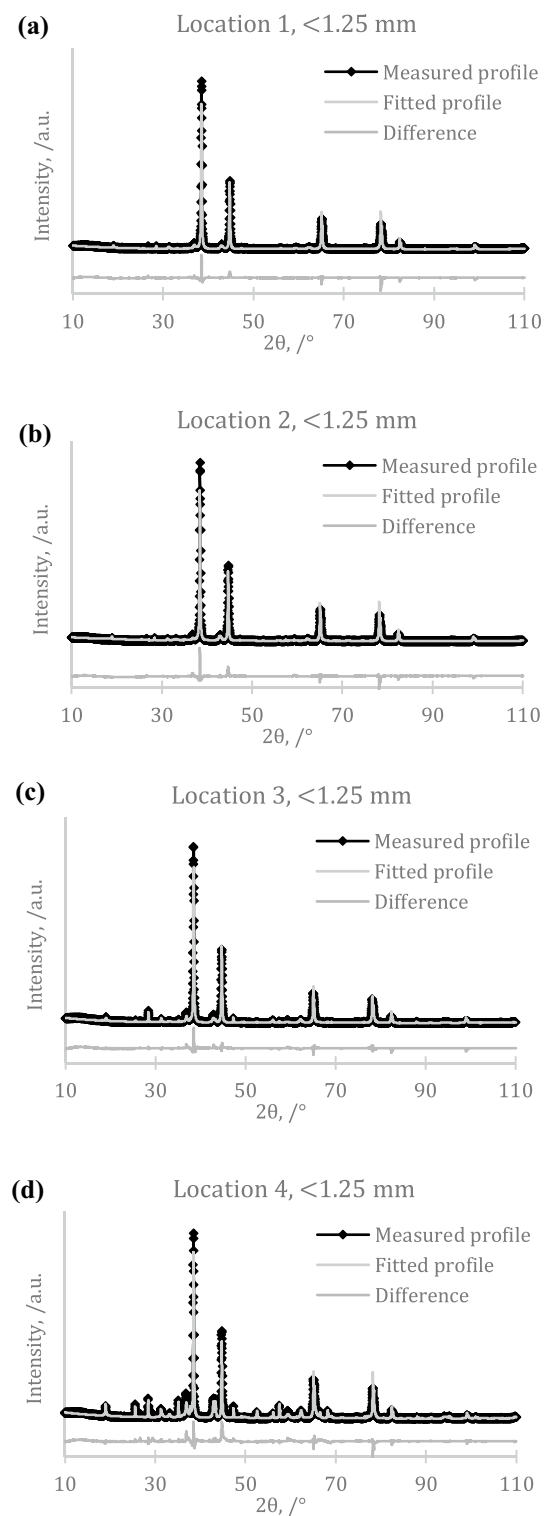

Fig. 8 XRD diffractograms of dross samples collected from Charge Y after being ring milled, where the measured profiles (black curve with diamonds), fitted profiles by using the Rietveld Method (light gray curve), and the difference between the measured and fitted profiles (dark gray curve) are plotted in **a–d** for the smallest fraction (< 1.25 mm) at Location 1 to Location 4, respectively

Table 4 Phase distribution for Charge Y from Location 1 to Location 4 for the smallest fraction (< 1.25 mm) of the ring milled dross samples calculated by the Rietveld Method

Phase	Phase distribution from loc. 1 to 4, /wt.%			
	Loc. 1	Loc. 2	Loc. 3	Loc. 4
Aluminum, Al	**80.8**	**75.3**	**69.0**	**51.5**
Magnesium oxide, MgO	8.6	9.8	18.7	14.4
Spinel, $MgAl_2O_4$	0.9	0.7	2.0	0.7
Defect spinel, $Mg_{0.388}Al_{2.408}O_4$	6.6	8.9	–	13.0
Aluminum oxide, Al_2O_3	1.0	1.6	3.7	14.6
Sodium aluminum oxide, $NaAl_{11}O_{17}$	0.0	0.1	0.3	0.3
Oxide content, total	**17.2**	**21.2**	**24.8**	**43.0**
Aluminum nitride, AlN	1.1	2.8	3.0	2.6
Silicon, Si	1.0	0.8	3.2	3.0

Bold indicates the significance difference between metallic and oxide, as well as having the other non-metallic compounds separately

Table 5 Phase distribution for Charge Z from Location 1 to Location 4 for the smallest fraction (< 1.25 mm) of the ring milled dross samples calculated by the Rietveld Method

Phase	Phase distribution from loc. 1 to 4, /wt.%			
	Loc. 1	Loc. 2	Loc. 3	Loc. 4
Aluminum, Al	**56.2**	**31.7**	**20.5**	**17.9**
Magnesium oxide, MgO	6.9	3.0	2.8	24.4
Spinel, $MgAl_2O_4$	4.0	0.6	4.5	0.5
Defect spinel, $Mg_{0.388}Al_{2.408}O_4$	2.2	29.1	12.5	23.1
Aluminum oxide, Al_2O_3	17.9	20.5	54.2	23.8
Sodium aluminum oxide, $NaAl_{11}O_{17}$	4.8	3.2	0.9	4.5
Oxide content, total	**35.8**	**56.4**	**74.8**	**76.4**
Aluminum nitride, AlN	7.5	11.6	4.6	5.4
Silicon, Si	0.5	0.4	0.6	0.4

Bold indicates the significance difference between metallic and oxide, as well as having the other non-metallic compounds separately

Comparison Between Ring Milling and Cryomilling

The differences between the ring milling and cryomilling pulverizing processes could potentially influence the phase distribution in the final pulverized samples. In light of this, one dross sample from the < 1.25 mm fraction of a third charge, i.e., Charge X, was milled using both ring milling and cryomilling, see Table 8. As seen from the table, both the metallic Al and the oxide contents were fairly similar for both techniques.
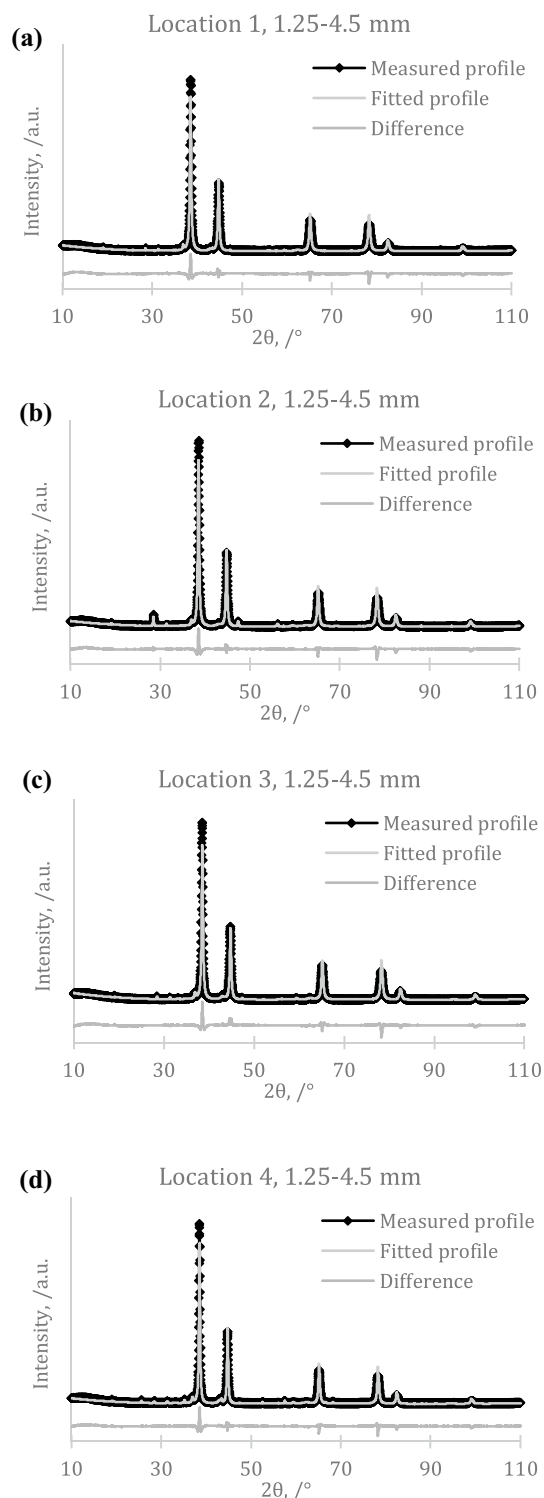
Fig. 9 XRD diffractograms of dross samples collected from Charge Y after being cryomilled, where the measured profiles (black curves with diamonds), fitted profiles by using the Rietveld Method (light gray curve), and the difference between the measured and fitted profiles (dark gray curve) are plotted in (**a–d**) for the mid-fraction (1.25–4.5 mm) at Location 1 to Location 4, respectively

Table 6 Phase distribution for Charge Y from Location 1 to Location 4 for the mid-fraction (1.25–4.5 mm) of the cryomilled dross samples calculated by the Rietveld Method

Phase	Phase distribution from loc. 1 to 4, /wt.%			
	Loc. 1	Loc. 2	Loc. 3	Loc. 4
Aluminum, Al	**88.1**	**86.3**	**85.2**	**81.7**
Magnesium oxide, MgO	4.5	6.4	7.2	7.8
Spinel, $MgAl_2O_4$	0.1	0.2	0.1	0.2
Defect spinel, $Mg_{0.388}Al_{2.408}O_4$	1.6	1.9	2.5	3.1
Aluminum oxide, Al_2O_3	0.5	0.3	0.3	4.3
Sodium aluminum oxide, $NaAl_{11}O_{17}$	2.9	0.0	2.1	0.00
Oxide content, total	**9.5**	**8.8**	**12.3**	**15.4**
Aluminum nitride, AlN	1.8	2.3	1.9	2.3
Silicon, Si	0.6	2.7	0.7	0.6

Bold indicates the significance difference between metallic and oxide, as well as having the other non-metallic compounds separately

Table 7 Phase distribution for Charge Z from Location 1 to Location 4 for the mid-fraction (1.25–4.5 mm) of the cryomilled dross samples calculated by the Rietveld Method

Phase	Phase distribution from loc. 1 to 4, /wt.%			
	Loc. 1	Loc. 2	Loc. 3	Loc. 4
Aluminum, Al	**82.3**	**73.5**	**57.2**	**54.9**
Magnesium oxide, MgO	5.5	3.6	2.3	17.4
Spinel, $MgAl_2O_4$	1.0	12.5	2.4	0.9
Defect spinel, $Mg_{0.388}Al_{2.408}O_4$	6.0	5.5	10.9	12.7
Aluminum oxide, Al_2O_3	3.1	2.5	23.7	10.9
Sodium aluminum oxide, $NaAl_{11}O_{17}$	0.0	0.1	0.1	0.1
Oxide content, total	**15.6**	**24.1**	**39.4**	**41.9**
Aluminum nitride, AlN	1.7	2.0	2.1	3.0
Silicon, Si	0.5	0.4	1.4	0.2

Bold indicates the significance difference between metallic and oxide, as well as having the other non-metallic compounds separately

Table 8 Phase distribution of the analyzed Al white dross sample (<1.25 mm fraction, Charge X.) pulverized by both ring milling (Case Study A) and by cryomilling (Case Study B)

Phase	Case Study A Ring milling, /wt.%	Case Study B Cryomilling, /wt.%
Aluminum, Al	**25.4**	**28.4**
Magnesium oxide, MgO	14.9	18.0
Spinel, $MgAl_2O_4$	1.3	0.1
Defect spinel, $Mg_{0.388}Al_{2.408}O_4$	19.0	29.8
Aluminum oxide, Al_2O_3	34.5	18.7
Sodium aluminum oxide, $NaAl_{11}O_{17}$	0.8	0.3
Oxide content, total	**70.5**	**66.9**
Aluminum nitride, AlN	1.5	3.5
Silicon, Si	2.6	1.2

Bold indicates the significance difference between metallic and oxide, as well as having the other non-metallic compounds separately

in the metallic Al in the sieve. Furthermore, it allowed for a systematic and reproducible way of dross sampling and was therefore seen as well suited for the task.

During the development of the sampling procedure, several steps were assessed, testing different approaches, e.g., (i) how and by what the sieve should be coated before being introduced into the bath, (ii) how deep the sieve should be submerged, (iii) how the sieve should be shaken after sample collection, and (iv) how many times the sieve should be shaken.

(i) Boron nitride was used for coating the sieve between each sampling and proved to be an essential step to avoid sticking of the metal to the stainless-steel sieve and occasionally even clogging the sieve. Both BN paint and spray were tested, but due to the viscosity of the paint, it was not as easily applied between each sampling as the spray.

(ii) To avoid a too large momentum when submerging the sieve into the molten metal bath, it was established that submerging the sieve just under the surface and moving it upwards toward the surface minimized the amount of metallic Al collected in the sieve during dross sampling.

(iii) For a successful sampling of the dross, it was noted that even more of the metallic Al collected in the sieve had to be drained. The sieve was therefore shaken with a gentle force both horizontally and vertically.

(iv) Shaking the sieve also proved to be an essential step that had to be fine-tuned to secure that the metallic Al did not solidify in the sieve, causing clogging. In regard to the time available, the sieve was shaken first

Discussion

Sampling Equipment and Procedure

It has been reported in the literature that dross is a challenging material to study due to its heterogeneity [22, 24]. The sieve design and the long handle assured, however, successful dross sampling from different locations in the holding furnace. It also allowed the metallic Al to quickly drain off and thereby leaving the oxide particles entrained

three times horizontally and then three times vertically, giving the best possible dross sample with a minimum content of metallic Al.

Sample Preparation and Analyses

Under the present processing conditions, both ring milling and cryomilling proved to be efficient techniques to promote particle size reduction of dross samples of different fractions for further quantitative analysis by XRD. For larger size fractions, the cryomilling was superior as it made the Al brittle and, hence, possible to mill.

When comparing the milling techniques adopted in the present study, it should be noted that the processing temperatures are different, i.e., ambient temperature versus cryogenic temperature. The milling dynamics are also different, with the driving force for ring milling being frictional forces and external impact forces for cryomilling. It was, however, demonstrated that despite these differences, the distribution of phases for the smallest fraction (< 1.25 mm fraction), including the metallic Al content, was of a comparable magnitude even if the softness and ductility of metallic Al were a challenge during ring milling.

XRD was chosen for analyzing the sieved and milled samples as the technique produces clear and unambiguous results. Combined with the TOPAS software and the ICDD-4 + PDF database, it becomes both a powerful and rapid technique capable of quantifying the phases present in the dross. It should, however, be noted that small crystalline structures that are present only in trace amounts may be undetected by the XRD readings.

The two analyzed charges, i.e., Charge Y and Charge Z, showed correlating results with respect to the phases present in the dross samples. The decrease of the metallic Al concentration from Location 1 to Location 4 as the oxide content increased was also the case for both charges. It was also established that the larger dross particles contain higher concentrations of metallic Al which agrees well with literature findings [24]. In view of this, the hypothesis that the sampling tool and procedures adopted secure a consistent collection of dross samples with a high degree of reproducibility is strengthened.

Industrial Dross Sampling vs. Present Procedure

The industrial dross sampling procedure considers only the total amount of dross generated during one skimming session and not the chemical composition of the dross. By introducing a sampling tool, as well as methodologies for sampling, pulverization, and quantitative analysis, it is believed to be possible to systematically study (i) the Al white dross formation and (ii) the phase distribution between metallic Al and oxides at an industrial scale. This, in turn, is believed to

give the industry further options and improved possibilities to control their generation of Al white dross and identify specific parameters to increase their total metallic Al yield.

Summary and Conclusion

Aluminum white dross is classified as a hazardous waste that generates toxic gases in contact with humidity and/or water. A burden on the environment is also recognized due to the large amounts of waste generated every year that must be transported and treated before being partly recycled or, in some cases, landfilled. In response to this, the present work has investigated the influence of standard furnace operations on the characteristics of the generated dross. A sampling tool (sieve) was designed to collect representative dross samples directly from the molten Al melt in the casthouse holding furnace. The tool was used together with developed step-by-step procedures for pulverization, XRD analyses, and verification of different properties of the dross.

Based on the presented and discussed results, it is evident that the designed sieve, as well as the method developed for its use, secures representative dross samples. It was also established that ring milling (< 1.25 mm fraction) and cryomilling (1.25–4.5 mm fraction) made it possible to prepare homogeneous powders for further quantitative XRD analysis containing both the brittle oxides and the soft Al. By refinement/optimization of standard process operations, it is believed that the Al industry will benefit from the outcome of the present study.

Future Work

Aluminum white dross samples generated during the production of Al alloys 1370 (> 99.7% pure Al) and 5182 (AlMg4.5Mn0.4) will be collected using the developed sampling tool, from the casthouse holding furnaces at the same industrial site as where the current sampling campaigns have been performed. The collected dross will be cooled in air and in protective atmospheres to evaluate the inhibiting effects that the protective atmospheres may have on the oxidation rate, as well as how it influences the dross morphology. The influence of the Mg concentration in alloy 5182 on the oxidation process and dross generation will also be investigated. In the future work, the method described in the present paper will also be followed for dross sample preparation (pulverization of three fractions, i.e., < 1.25 mm, 1.25–4.5 mm and > 4.5 mm, metallographic characterization, and quantitative image analyses) and cross-validated by XRD analysis.

Data Availability The data used to support the findings included in this publication can be accessed on request.

Declarations

Conflict of interest The authors declare that they have no conflict of interest.

References

1. Sverdrup HU, Ragnarsdottir KV, Koca D (2015) Aluminium for the future: modelling the global production, market supply, demand, price and long term development of the global reserves. Resour Conserv Recycl 103:139–154. https://doi.org/10.1016/j.resconrec.2015.06.008

2. Mahinroosta M, Allahverdi A (2018) Hazardous aluminum dross characterization and recycling strategies: a critical review. J Environ Manage 223:452–468. https://doi.org/10.1016/j.jenvman.2018.06.068

3. Shi R, Miao J, Avey T, Luo AA (2020) A new magnesium sheet alloy with high tensile properties and room-temperature formability. Sci Rep 10:10044. https://doi.org/10.1038/s41598-020-67161-9

4. Banhart J, Chang CST, Liang Z et al (2010) Natural aging in Al-Mg-Si alloys—a process of unexpected complexity. Adv Eng Mater 12:559–571. https://doi.org/10.1002/adem.201000041

5. Steglich J, Friedrich B, Rosefort M (2020) Dross formation in aluminum melts during the charging of beverage can scrap bales with different densities using various thermal pretreatments. JOM 72:3383–3392. https://doi.org/10.1007/s11837-020-04268-4

6. Solem CKW, Ekstrøm KE, Tranell G, Aune RE (2020) Evaluation of the effect of CO_2 cover gas on the rate of oxidation of an AlMgSi alloy. In: Tomsett A (ed) Light metals 2020. Springer International Publishing, Cham, pp 1141–1147

7. Takuya Y, Kenya K, Komarov SV et al (2020) Evaluation of aluminum dross generation rate during mechanical stirring of aluminum through model experiment and numerical simulation. Metall Mater Trans B 51:1836–1846. https://doi.org/10.1007/s11663-020-01842-8

8. Johansen I, Strømhaug SI (2016) Energy control in primary aluminium casthouse furnaces. In: Sadler BA (ed) Light metals 2013. Springer International Publishing, Cham, pp 935–939

9. Taylor JA, Prakash M, Pereira GG, et al (2010) Predicting dross formation in aluminium melt transfer operations. Materials science forum. https://www.scientific.net/MSF.630.37. Accessed 2 Nov 2018

10. Drouet MG, Handfield M, Meunier J, Laflamme CB (1994) Dross treatment in a rotary arc furnace with graphite electrodes. JOM 46:26–27. https://doi.org/10.1007/BF03220691

11. Ünlü N, Drouet MG (2002) Comparison of salt-free aluminum dross treatment processes. Resour Conserv Recycl 36:61–72. https://doi.org/10.1016/S0921-3449(02)00010-1

12. Tsakiridis PE (2012) Aluminium salt slag characterization and utilization—a review. J Hazard Mater 217–218:1–10. https://doi.org/10.1016/j.jhazmat.2012.03.052

13. Das BR, Dash B, Tripathy BC et al (2007) Production of η-alumina from waste aluminium dross. Miner Eng 20:252–258. https://doi.org/10.1016/j.mineng.2006.09.002

14. Hu K, Reed D, Robshaw TJ et al (2021) Characterisation of aluminium black dross before and after stepwise salt-phase dissolution in non-aqueous solvents. J Hazard Mater 401:123351. https://doi.org/10.1016/j.jhazmat.2020.123351

15. Lashchev VYA, Rybinov VA, Terziyan PG (1969) Device for sampling metal and slag. Metallurgist 13:636–637. https://doi.org/10.1007/BF00734620

16. Abdulkadir A, Ajayi A, Hassan MI (2015) Evaluating the chemical composition and the molar heat capacities of a white aluminum dross. Energy Procedia 75:2099–2105. https://doi.org/10.1016/j.egypro.2015.07.326

17. David E, Kopac J (2012) Hydrolysis of aluminum dross material to achieve zero hazardous waste. J Hazard Mater 209–210:501–509. https://doi.org/10.1016/j.jhazmat.2012.01.064

18. Hwang J-Y, Huang X, Xu Z (2006). Recovery of metals from aluminum dross and saltcake. J Miner Mater Charact Eng 5(1):47–62. https://doi.org/10.4236/JMMCE.2006.51003

19. Capuzzi S, Timelli G (2018) Preparation and melting of scrap in aluminum recycling: a review. Metals 8:249. https://doi.org/10.3390/met8040249

20. Meshram A, Gautam D, Singh KK (2020) Recycling of white aluminium dross: production of potash alum. Trans Indian Inst Met 73:1239–1248. https://doi.org/10.1007/s12666-020-01973-1

21. Kvithyld A, Bao S, Nordmark A et al (2014) Development of a sampling device for furnace dross. In: Grandfield J (ed) Light metals 2014. Springer International Publishing, Cham, pp 931–935

22. Gomez A, Lima NB, Tenorio JAS (2008) Quantitative analysis of aluminum dross by the rietveld method. Mater Trans 49:728–732. https://doi.org/10.2320/matertrans.MRA2007129

23. Dutta BN (1962) Lattice constants and thermal expansion of silicon up to 900°C by X-ray method. Physica Status Solidi (b) 2:984–987. https://doi.org/10.1002/pssb.19620020803

24. Kudyba A, Akhtar S, Johansen I, Safarian J (2021) Aluminum recovery from white aluminum dross by a mechanically activated phase separation and remelting process. JOM 73:2625–2634. https://doi.org/10.1007/s11837-021-04730-x

Publisher's Note Springer Nature remains neutral with regard to jurisdictional claims in published maps and institutional affiliations.

Authors and Affiliations

Cathrine Kyung Won Solem[1] [ID] **· Stefano Deledda[2] · Gabriella Tranell[1] · Ragnhild E. Aune[1]**

[1] Department of Materials Science and Engineering, Norwegian University of Science and Technology (NTNU), Alfred Getz Veg 2, 7034 Trondheim, Norway

[2] Department for Hydrogen Technology, Institute for Energy Technology (IFE), Instituttveien 18, 2007 Kjeller, Norway